Report Title

Farah Akhtar
Farah.akhtar@colorado.edu

Submitted in partial fulfillment of the requirements of

ECEN 5004
Environmental Signal Processing

Department of Electrical and Computer Engineering
University of Colorado at Boulder

December 16, 2017

ABSTRACT

GNSS signals have found varied applications in altimetry and scatterometric observations over ocean, ice, sea ice and land to model various atmospheric parameters. In view of the growing interest in the scientific community towards identification and monitoring of wetlands, we see an opportunity in using CYGNSS data for applications in wetland identification. In this paper, we define the main data product of CYGNSS as a mapping from the space to Delay-Doppler Map coordinates. We also present studies that demonstrate the feasibility of use of CYGNSS data for application in monitoring of flat water and estimation of vegetation cover height. We present a three-parameter model designed for inversion from measurements using Interference Pattern Technique. Finally, we present a brief error analysis and a Cramer-Rao bound on the achievable temporal resolution for the given measurements.

1.0 INTRODUCTION

The Global Navigation Satellite System (GNSS) signals have been recognized by the world scientists as signals of opportunity to be used for Earth Remote Sensing for more than two decades. As of 2016, there were around 90 operational satellites in orbit, from several systems all over the globe, transmitting GNSS signals in the L1 band and, hence, providing almost global coverage of most ocean and land surface at a reasonably high temporal resolution in this frequency band. While there are mounting concerns about the increasing RF noise floor, these numbers are expected to increase to about 120 in the next five years based upon the various GNSS missions expected to launch. In any case, it is indeed safe to say that the GNSS signals will be available for remote sensing with relatively low-cost, small form non-cooperative receivers due to the presence of these extensive Global Navigation Systems.

The potential of GNSS Reflectometry as a technique for altimetric observation was first suggested by Martín-Neira in 1993[1]. Initially, ground based geodetic GNSS receivers at low elevation angles were used to infer changes in soil moisture, snow depth and vegetative growth from changes in interference patterns due to multipath propagation. Since then, there have been several missions that have demonstrated the feasibility and varied applications for the GNSS signal observation from aircrafts and space. The applications of the first few missions for this kind of observations focused on characterization of sea surface roughness, salinity, permittivity and wind dynamics over sea. Over time, the applications have extended to sea ice characterization, observation of soil moisture and other land and hydrological applications. The first mission to perform remote sensing measurements using GNSS signals from space was the the UK-DMC, the UK Disaster Monitoring Constellation. Several aircraft and space missions have resulted in the demonstration of feasibility in monitoring wind measurements over ocean[2] , characterization and monitoring of various ocean and land features[3] and snow characterization using volumetric scattering [4].

While there is reasonable global coverage by the GNSS satellites, the observations from these missions were deemed inadequate on two accounts as identified by the global scientific community. The efforts to address these very issues, eventually, led to the selection and launch of the Cyclone Global Navigation Satellite System (CYGNSS) by NASA in December, 2016. The limitations that were to be addressed by CYGNSS can be described as follows:

1. Most of the climate and weather observations that are assimilated into current weather models comes from geostationary satellites and polar orbiting satellites. Conventional polar orbiting satellites have a wide swath and do not provide enough temporal resolution to observe and understand the rapid process of genesis and intensification of Tropical Cyclones.
2. Most of the conventional remote sensing signals are obscured and not observed during rainfall. Therefore, observations during precipitation events, especially in the eye-wall of tropical cycles where intense precipitation occurs, are not available.

CYGNSS seeks to address both these limitations with the launch of a new constellation of 8 satellite observatories. The availability of 8 satellites in a Low-Earth Orbit at an inclination of 35° results in a temporal resolution of observation to an average of 5-7 hours for a given location in orbit. In addition, these receivers observe the Earth at a relatively long L1-band wavelength of 19.02 cm, making observations unbiased by the presence of precipitation. While the primary science goals of CYGNSS were focused on observation of ocean surface, retrieval of wind speeds on the ocean and operational forecasts and development of hurricanes, there has been a growing set of applications for the data focused towards land, snow and ice observation. More recently, as motivated by the International Panel for Climate Change (IPCC), the scientific community has been developing applications for detection, classification and monitoring of wetlands. There is a growing interest in asserting feasibility and demonstrating applications of the CYGNSS data for detection and monitoring of wetlands.

Wetlands monitoring applications have attracted attention from the scientific community for as long as the satellite data became available since the 1990s. Various satellite data products have been used for detection, mapping and monitoring of wetlands. [5] [6] [7] More recently, Nghiem

et. al. [8] have used GNSS data collected from an aircraft flight campaign to develop a database of land and ocean features, using inundated rice fields as a case study for vegetated wetlands. Their study provides insights into the differences between reflected power (Doppler-Delay Maps, explained later) and Signal-to-Noise (SNR) ratios for the GNSS signals for ocean observations as well as topographical features observed over land including mountains, lakes and wetlands. While their study is insightful from the point of view of a statistical model development, it requires a statistically representative sample set of observations for a given wetland before it can be positively identified and characterized. We describe their achievements and limitations in more detail in the next sections. It is worth noting here that their study needs supplemental data and parametric information for successful classification and monitoring of wetlands.

In this paper, we discuss the lessons gained from earlier studies by way of using GNSS signals for various applications. We also take a deeper look at the published or developing models for wetlands, taking lessons from their strengths and considering alternatives to address their limitations. Based on the database development undertaken by earlier studies, we propose binary hypothesis testing to identify regions that have a potential for classification as wetlands. The hypothesis test is based upon the relative difference (SNR ratio) of the successive land and wetland permittivity ratios as satellite footprint crosses these feature boundaries. Next, we propose a parametric model that can be inverted to specify surface height, vegetation cover height, fractional water coverage in a CYGNSS pixel and the salinity and temperature related characteristics of the wetland. We propose the use of Interferometric Pattern Technique (based on measurement of phase delay) to find the roughness of the wetland surface due to floating vegetation or surface waves due to wind fetch. We also propose to measure the Brewster's angle which can be inverted to obtain the dielectric constant of the wetland water. This information may be used to further identify the water for its transparency, salinity and temperature etc. Further, the presence of notches in the correlated reflected power can be used to identify presence and height of the canopy cover on the water surface.

In the next section, we briefly explain the physical principles behind the GNSS observations and the characteristics of the forward scattering pattern for the data to be useful for identification and classification of wetlands. In section 3, we detail the past work related to wetland monitoring and its limitations. In section 4, we present some earlier studies to demonstrate the feasibility of our

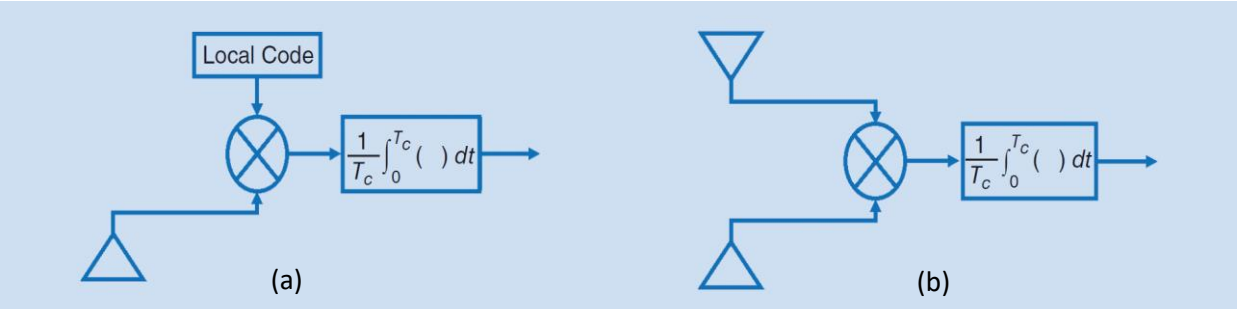

Figure 1: The illustration of the working principle of r-GNSS and i-GNSS receivers. In (a), the r-GNSS receiver uses a locally generated PRN code. In (b), the i-GNSS receiver uses direct and reflected copies of the signal to generate data products.

approach outlined in Section 5. In section 5, we propose the theoretical model for inversion of the CYGNSS data to identify parameters for wetlands. Finally, we conclude by presenting a brief analysis of the error characteristics of our model and discuss the limitations that may confound it.

2.0 Physical Principles for GNSS-R Remote Sensing

The main product of the GNSS receivers is a descriptor of the state of the reflected surface called the Delay-Doppler map (DDM). It is calculated as a function of delayed and doppler-shifted copies of the original (directly received or locally generated PRN-code) signal by integration over an integration time (Illustrated in figure 1). If the observed surface (of the Earth) is to be considered as a spherical surface in physical coordinates, each pixel on the surface (xy)- space can be mapped into a Delay-Doppler (DD) $(\Delta\tau, \Delta f_D)$ domain and each of these points has a power associated with it. The power associated with each pixel in the DD domain is, in fact, a sum of two different points over the observed surface, leading to an ambiguity in the deconvolution of the DDM. However, the central line of no ambiguity may be used for this kind of deconvolution. Figure. 2 illustrates the mapping from (xy) to DD domain space. Figure 1(a) shows the physical surface as a combination of (green) equi-range or equi-delay lines and (red) equi-doppler hyperbolae forming the surface. Figure 1(b) shows the non-linear (and ambiguous) mapping from the (xy) space to the characteristic horseshoe shaped DDM. The shape is characterized by the brightest pixels lying around the line marked A′O′B′ mapped from the unambiguous line (of single pixels). The blue area in the background corresponds to the non-intersecting equi-range and equi-doppler lines. For all the pixels in DDM, the intensity of the pixel is proportional to the power scattered by the pair of pixels locating symmetrically on either side of the line AB.

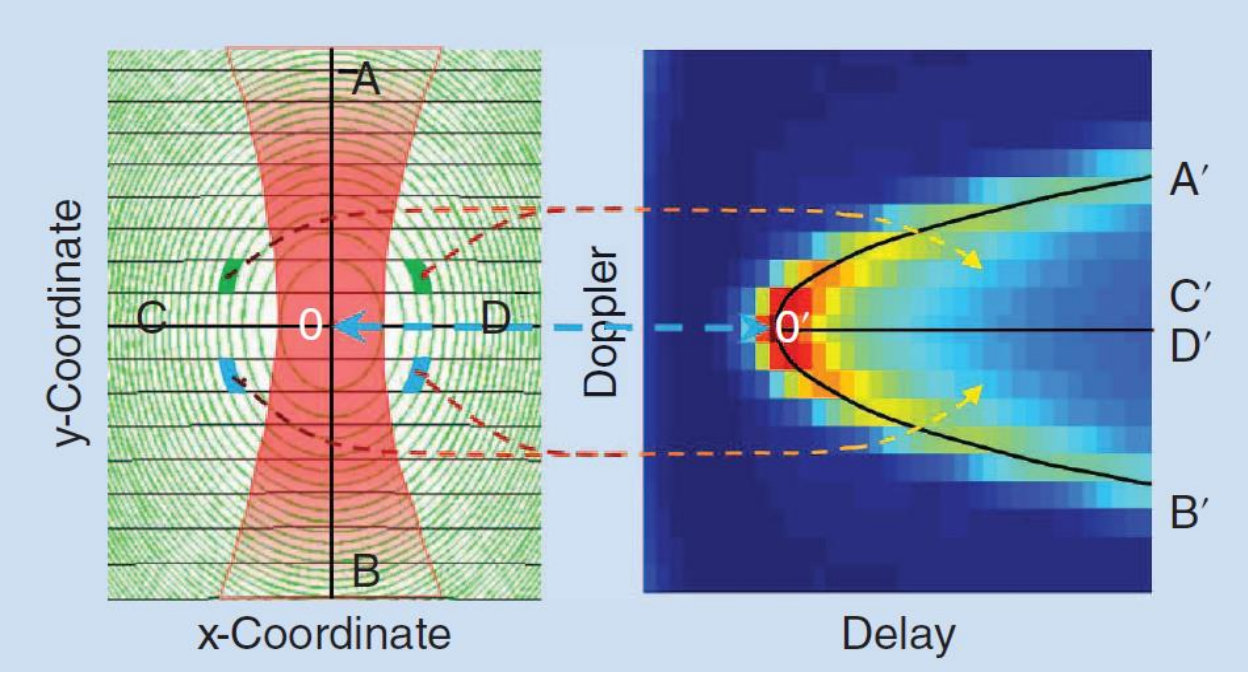

Figure 2: Illustration of equi-range and equi-doppler signal bins and a Delay Doppler Map.

The GNSS signal illuminating the Earth's surface is a relatively low-power signal. Therefore, acquiring the reflected signal with a reasonably high SNR is a challenge. This is the reason that the CYGNSS observatories use the direct signal from the zenith-facing antenna to calculate the specular points to latch with for potential Doppler Delay Map (DDM) calculations. Only the specular points observed by the nadir-looking antenna that meat a certain peak power threshold are used to calculate the DDMs. Also, the receivers use the scattered signal over a limited angular zone (called the "glistening zone") around the specular direction to obtain a cross-correlation of the reflected signals with the direct signals from the GNSS transmitters. This cross-correlation is obtained over an interval of time called the 'coherent integration time' which is chosen as a trade-off between maximizing SNR and minimizing the multiplicative (Speckle) noise in the DDM calculations.

The coherent integration time is governed by the correlation time τ_{cor} for which the reflected copies of the signal can build up into the coherent integration term to calculate the DDM. Choosing a small integration time might result in the correlated output being too low in SNR to estimate the signal characteristics from the reflected copies. On the other hand, a long integration time does not improve SNR any more than incoherent summation of independent samples. The coherent integration time is also what determines the size of the Doppler zone, thus determining the pixel size (or spatial resolution) of the observed surface corresponding to the given DDM.

In radars, the ambiguity function provides a measure of similarity between the signal and a delayed, doppler-shifter version of it. Therefore, the DDM can also be thought of as a function of the ambiguity function of the GNSS-R receiver. The calculation of the DDM can be summarized into the following bistatic radar equation as given in [9]:

$$\langle |Y(\tau, f_d)|^2 \rangle = \frac{\lambda^2 T_i^2}{(4\pi)^3} P_t G_t \iint_G \frac{G_r}{R_t^2 R_r^2} \chi^2(\tau, f_d)\, \sigma_0 \; dS \qquad (1)$$

where T_i is the coherent integration time, $P_t G_t$ is the transmitter's Effective Isotropic Radiated Power, G_r is the receiver antenna gain pattern, R_t and R_r are distances between the nominal specular point and the transmitter/ receiver, respectively, χ^2 is the Woodward Ambiguity Function (WAF) which describes the range and Doppler selectivity of the coherent radar, σ_0 is the normalized bistatic radar cross section (BRCS) of the rough surface, which gives a portion of the scattered power carried by the outgoing plane wave in a specific direction, while the unit surface is being illuminated by the unit wave incoming in another direction.

More specifically, the WAF can be approximated as the square product of the two functions representing equi-delay annulus zone $\Lambda(\Delta\tau)$ and the function representing equi-doppler-frequency zone, $S(\Delta f)$. The width of the function $\Lambda(\Delta\tau)$ is itself proportional to the width of the PRN chip code whereas the function $S(\Delta f)$ is related to the inverse of the coherent integration time and $D(\rho)$ is the antenna radiation pattern:

$$\chi^2(\tau, f_d) = \; D^2(\rho)\, \Lambda^2(\Delta\tau)\, |S(\Delta f)|^2 \qquad (2)$$

The Bistatic Radar Cross Section (BRCS) can be modeled by one of the many EM model approximations. The GNSS-R receiver in CYGNSS uses the Geometric Optics limit of Kirchhoff approximation. The term in equation (1) above does not fully describe the complete surface to

DDM space mapping in that it only represents the diffuse scattering component of the reflecting surface and ignores the specular reflection component. To make up for that, an additional term representing the specular reflection component can be added to it. This term is what describes the sharp peak of the DDM centered at the point corresponding to the nominal specular point of the reflecting surface against the shallow pedestal of values of power as given in equation (1) at all other points in the glistening zone. The term is given below as:

$$\langle |Y(\tau, f_d)|^2 \rangle_{spec} = |Y_0(\tau, f_d)|^2 |\Re|^2 e^{(-8\pi^2 \sigma_h^2 cos^2\theta / \lambda^2)} \qquad (3)$$

where $\Re$ is the Fresnel's Reflection Coefficient and the exponential term is the factor accounts for the loss of spatial coherence due to the presence of some relatively weak surface roughness.

All the secondary data products of the CYGNSS receivers are derived from the various aspects of the DDM power area, volume, peak delay, tail shape or slope characteristics. These include the Mean Square Slope (MSS) product inverted to wind speed measurements, delay of the peak power related to phase delay measurements and several other secondary and tertiary data products.

3.0 Previous Work in Wetland Monitoring and Opportunities for Improvement

As already mentioned, all the satellite data sets collected since the launch of satellite missions in the last decade of 20th century and, later, most of the data for GNSS missions has been used towards the applications for wetland monitoring, in terms of their mapping and monitoring. Published in 1996, the International Geosphere-Biosphere Programme – Global Analysis, Interpretation and Modelling report[10] evaluated advantages and limitations of the various remote sensing methods for wetland mapping. In the given report, as well as more recently, in the report[11] for the International Panel for Climate Change (IPCC), the importance of wetlands as key drivers for emission of methane and the necessity for their mapping and dynamic classification and monitoring was recognized again and highlighted for the scientific community.

Specifically, the Japan Aerospace Exploration Agency (JAXA) aims to use L band SAR for long term systematic observations of the tropical and boreal wetlands. Similarly, [12] have used techniques for flood detection, mapping and measurement as well as space-based measurements of river runoff that can be adapted for applications in wetland observation. While there has been some success in better monitoring and understanding of wetlands since the 1980s and onwards, one major limitation of even the more recent observations pertains to the limited temporal resolution of the observed wetlands. The highest temporal resolution that could be achieved by the satellite observations was about 6 weeks, for example for ALOS-2 mission. Another limitation of the C-band SAR observation emerges from the short (5.6 cm) bandwidth which does not allow for uniform detection of forested or densely vegetated wetlands. CYGNSS mission provides an opportunity for better understanding of wetlands as the temporal resolution of observation increases to a few hours. In addition, as described in the next section in more detail, the phase delay measurement and observation in the L-band provides a unique opportunity for observation of flat water, and consequently, vegetated wetlands (because of their characteristically flat surface).

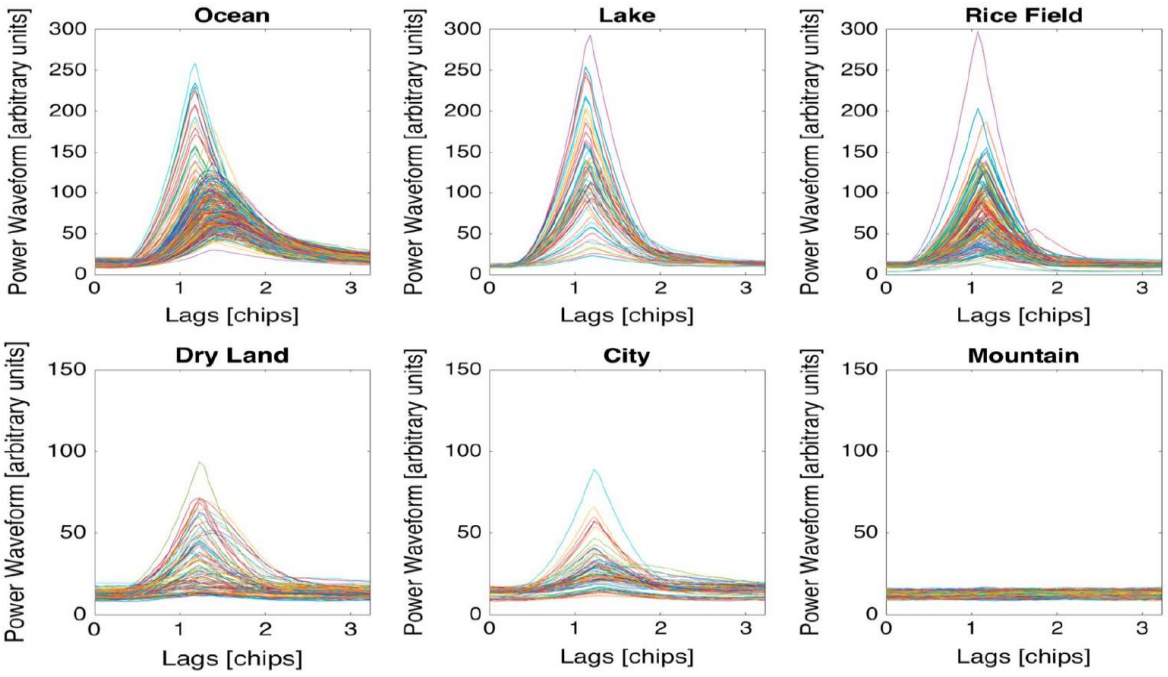

Figure 3: Measurements of the various waveforms of reflected power measured over different terrain classes for the flight campaign over Ebro River Delta.

[8] conducted a flight campaign over the Ebro River Delta in Spain to demonstrate the potential for observation of wetlands. During their flight campaign, they also observed the changes in wet surface extent in the Mississippi delta area and compared their observations with the ground truth data available from USGS gauges upstream and downstream of the observed wetlands and stream flow around the flood plain. Their study provides some useful insights regarding the current state of science in observation of wetlands as presented in context of observations from ocean and various land features. Figure 3 shows the various waveforms of reflected power measured over the different terrain classes during the campaign. While the observations of power (as represented by 2-dimensional DDMs in the figure) are insightful by way of building a database for the observations of certain land and water-based features, their statistical results (as presented in Table 1) are more useful in terms of application to a dynamic detection and inversion model for the wetlands.

	Difference in SNR_R/SNR_D (dB)		
Terrain Type	Mean	Median	Standard Deviation
Rice field-lake	−2.63	−2.45	2.04
Rice field-ocean	−1.53	−1.54	1.70
Rice field-dry flat land	4.16	3.61	2.68
Rice field-city	2.56	2.24′	2.66
Rice field-mountain	6.79	6.79	3.48

Table 1: Mean and Median SNRR/SNRD Difference Computed in Decibel (dB), Using the 1° Elevation Angle Binning Method, for Various Surface Classes When Compared to Rice Field in the Study Domain of the Catalonia Flight Campaign in Spain.[8]

The study in [8] was formulated such that the observations of SNR from a given land or water feature, for example, lake, mountain, ocean or city etc. were collected into statistical bins and their mean, median and variances calculated. As a second step, the observations were normalized based on incidence angle and it was verified that the data in the same incidence angle bins exhibited azimuthal symmetry. This resulted in their conclusion that the ratio of SNR for signals reflected from a pair of observed surfaces as the aircraft flew over the boundary between them converged in a statistical sense. For an example, the ratio of SNRs from the edge between land and wetland was more than 3dB and could also be characterized similarly for other boundaries. They proposed that this statistical convergence to a 3dB higher mean power being reflected from the wetland compared to dry land could be used to identify wetlands. They found that the strong forward scattered power from the flat-water wetlands could allow a distinctive identification of wetlands in spite of the attenuation due to vegetation.

While the results from the study are encouraging and demonstrate a possibility of detection of the edges around wetlands, there are limitations that make these observations unsuitable for use in space-based reflectometric identification. The study was conducted using aircraft with a GNSS-R receiver aboard and suggests that a nearly constant angle of incidence must be maintained a clear characterization of observed data for wetlands. While this may be possible, for a limited set of observations in the aircraft based or space-based observations, this is not a practical possibility for most of the observations. Even for CYGNSS, as for other low-earth orbit satellites, the angle of incidence may vary significantly from one pass to another. Also, the CYGNSS orbit do not follow the exact orbit over successive passes but instead, maintain an oscillating orbit in the 38°S to 38°N range. Therefore, it is possible to repeat the exact observation (and consequently, a similar angle of incidence) in about 14 days for a given CYGNSS receiver. Therefore, the advantage of having a high temporal resolution in the data is completely offset if we are to acquire a statistically useful and representative data set of observations over a given part of the globe to be observed and characterized. Still, it is possible to use such data for characterization of wetlands over a longer period of observation and then continue to improve the characterization and continued monitoring after initial identification and characterization.

4.0 Potential for use of Interference Pattern Technique and supporting studies

Given the limitations in the section above, we consider the various parameters in the signal power, delay and doppler frequency characteristics that can be used to better characterize wetlands, especially when they are vegetated and experience signal attenuation due to the presence of vegetation. In this regard, pay attention to the Phase Delay altimetry to develop a set of observables that can be used to estimate the parameters for a model suitable to model wetlands. While it has been recognized that phase delay altimetry can be very precise, it can also be very inaccurate even with small additive noise[13]. This leads to its efficiency and efficacy being best for very smooth surfaces only. For such smooth surfaces, experimental studies have been able to achieve altimetry measurement inversions with an accuracy of 1-2 cm [1] [14].

For application into observation of wetlands, this may be a positive thing. Marshlands and inundated fields are characterized by some amount of vegetation and very low amount of wind fetch. It is often observed that the wind-induced roughness can be damped down to a degree by

the vegetation, hence, presenting a flat surface for observation for reflected GNSS signals. However, there is some attenuation due to the presence of vegetation, which will attenuate the reflected signal in a given pixel of CYGNSS data proportional to the canopy cover and vegetation height. While there is a possibility to model the trees and plants within a wetland as separate dielectric cylinders within the reflective water surface, a first model can make use of an estimate of canopy height and percentage cover. This is exactly the measurement that can be obtained from the measurement of correlated reflected power from the given surface. The ration of the dielectric constants of multiple dielectric layers, like water and air in the case of a wetland, representing the surface being observed, can be detected by a measurement of the Brewster's angle[3]. The Brewster's angle can be inverted to the dielectric constant of the second layer observed besides air. This measurement presents useful results, not only for the detection of presence of water, but also helps estimate the water characteristics like salinity, biomass content and temperature as the dielectric constant varies. This measurement can be essential for monitoring changes in the wetland structure even after identification and characterization stages.

Interestingly, the presence of a third layer can also be detected from the presence of notches in the measurement of correlated reflected power. After the Brewster's angle is used to identify the second layer, presence of a notch can point at the presence of a third layer. The number of notches present in the reflected power spectrum increases with presence of more layers between the reflecting surface and the receiver. This characteristic of the signal has been used by [3] to establish a relationship between the number of notches and the height of the vegetation canopy. The number of notches is indicative of the layers of vegetation present from 60cm of layer height up to 3m of layer height. At about 3m of canopy height, the presence of lower layer, which in the case of wetland is the presence of water, cannot be detected any longer.

We use the studies discussed above as a demonstration that the principle that works for the given measurements can also work for the case of identification and characterization of wetlands. Whereas the measurement of phase delay has been used repeatedly to measure the surface height accurately, the Brewster's angle measurement for measurement of dielectric constant (of soil with some soil moisture content) and the number of notches used to characterize the vegetation height, these measurements have not been used in conjunction with identification and characterization of wetlands. We present the case here that it is possible for these measurements to be used as such for that purpose.

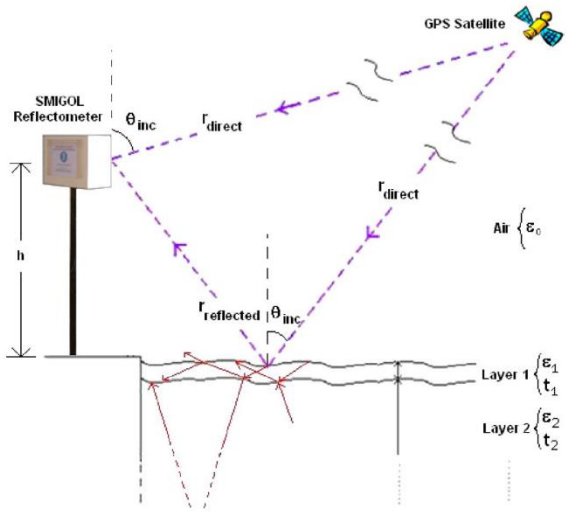

Figure 4: Illustration of the principle of doppler delay measurement used for a ground-based GNSS receiver.

5.0 Parametric Model based on Interference Pattern Inversion

We present a parametric model for the identification and characterization of wetlands. The model is proposed to have three parameters each of which is described in more detail below. Additionally, we describe how the inversion from the measurement space to parameter space is expected to proceed.

- *Phase Delay:*

The measurement of phase delay takes the form of the following equation:

$$\emptyset(t) = \emptyset(t_0) + e^{i\,k\,\Delta r(t)} \qquad (4)$$

where Δr is the change in r after t_0. A land- based receiver set up for such a measurement is illustrated in figure 4. This measurement is expected to be very precise because a change of a full 360° of phase results in a variation of only about on wavelength λ (~20cm) in the observable. This measurement reflects itself as a change in range (or delay) values in the DDM mapping. The measurement of phase delay can be very inaccurate with rough surfaces, however. This is because phase changes abruptly and unpredictably when reflected from diffuse scattering surfaces. Considering that our surface of interest is expected to have smooth surface characteristics for most of the time, we expect the variable to give us an inversion to the surface height measurements relative to the receiver. However, we are most interested to characterize the observe surface as a wetland instead of measuring its surface height. Therefore, we can formulate this variable as a binary hypothesis test for detection of absence of wetland. Since phase delay is sensitive to surface roughness, we will be able to receive very high specular reflections when the surface of water is smooth and completely useless measurement (or lack thereof) of phase delay if the reflecting surface is not flat water i.e. either it is a rough water surface or is a land feature. Therefore, it is possible to formulate the hypothesis for a threshold value of coherent phase delay measurements.

H1 = Observed surface is a smooth wetland/lake
H0 = Observed surface is a rough water surface or land.

Given a threshold value α, we choose H1 if surface brightness (or specular reflection term) is > α. We choose H0 if the surface brightness is diffuse (and specular reflection term is absent or too much smaller than α).

There is a possibility to get false positives for the calm lakes on any given pass. Similarly, there may be rare local wind conditions that may make the wetland surface rough. However, these characterizations can be improved over multiple passes. In addition, the other variables (described next) in combination with Δr may be useful in complete characterization of the wetland.

- *Brewster's Angle*

Measurement of Brewster's angle can be given by the following equation:

$$\theta_B = \arctan\left(\sqrt{\frac{\mu_{r2}.\varepsilon_{r2}}{\mu_{r1}.\varepsilon_{r1}}}\right) = \arctan\left(\sqrt{\frac{\varepsilon_{r2}}{\varepsilon_{r1}}}\right) \quad (5)$$

where μ_{r1} and μ_{r2} are the permeability values for each of the mediums in two layers above the observed surface and ε_{r1} and ε_{r2} are, respectively, the dielectric constant of the two layers. Given that the first layer in our case is air, we can use the Brewster's angle equation above to measure the dielectric constant ε_{r2} of the water being observed. Figure 5 shows a simulated plot of the interference power and the first notch corresponding to Brewster's angle for a bare soil moisture layer. [3] The Brewster's angle can then be inverted to get an estimate for the dielectric constant of the water layer being observed in case of wetlands observation.

As should be noted, the dielectric constant for water changes with temperature, salinity and biomass conditions of the wetland under observation. Therefore, the measurement of this variable alone, just like the phase measurement alone, may cause some ambiguity. However, together the two variables can ensure that the measured surface can be characterized successfully. For example, the specular brightness above a certain threshold accompanied by the measurement of a dielectric constant characteristic of a certain set of water bodies (say, brackish marshland), in combination, can provide a certain high level of confidence to the observations.

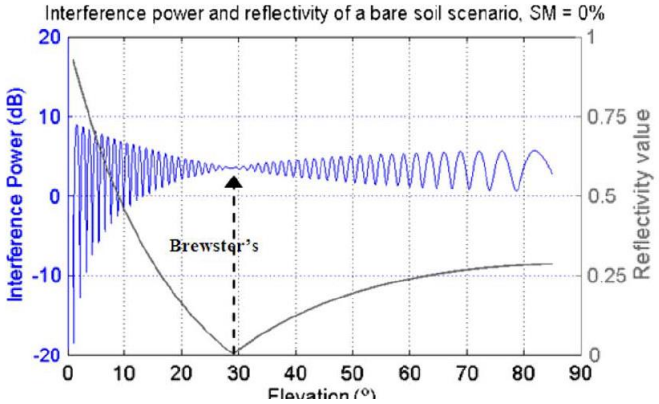

Figure 5: Simulated interference power received versus reflectivity for a soil-air layer. Note that the Brewster's angle position maches with the notch indicating the characteristics of the second layer.

- *Number of Notches in received Interference Power*

The number of zero values that the interference power (or reflectivity) of the surface achieves can be used as a count for the number of layers available after the first layer has been identified using Brewster's angle. It may be necessary to experimentally characterize further the kind and coverage of vegetation that gives a notch any given point. However, as experimentally proven in [3] and illustrated in figure 6, we can see that the presence of notches can be characterized as the number of layers where each increment in the vegetation height shows itself as an additional layer (and notch) in the spectrum. Figure 7 shows a plot of variation of reflectivity and observed notches for different heights of vegetation.

Another consideration in experimental evaluation, which may be different from the study in [3] is that the coverage of vegetation in the pixel being observed may not be even. While the

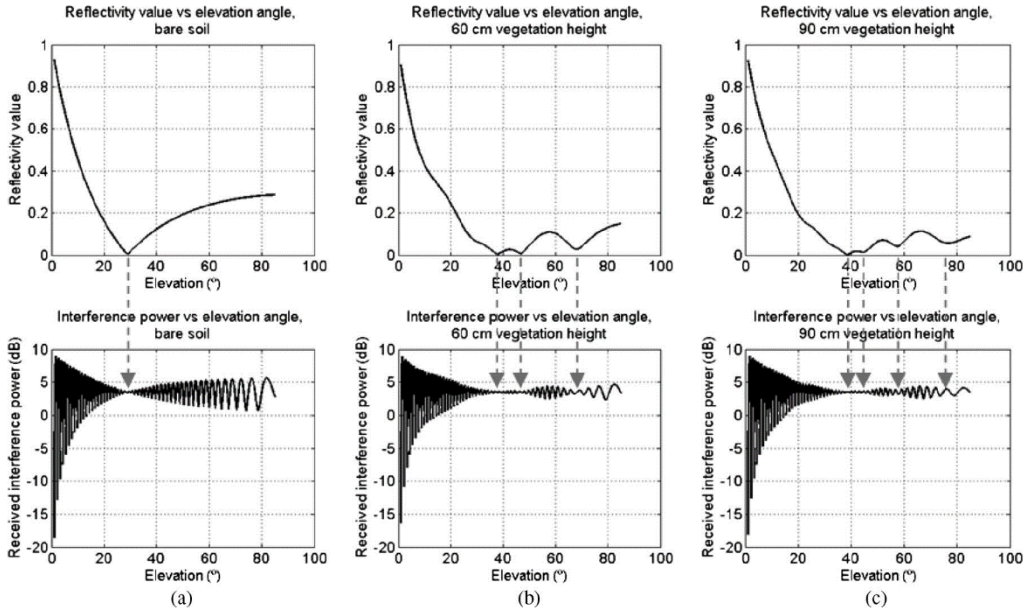

Figure 6: Simulated interference power received versus reflectivity. (a) Bare soil produces one notch, (b) 60-cm vegetation layer + soil layer produces notches, and (c) 90-cm vegetation layer + soil layer produces four notches. Note that first notch is notch is due to the Brewster's angle, but new notches appear due to oscillations in the reflectivity.

study referred above observed agricultural inundated land as a proxy for wetlands and consequently, was able to characterize a nearly even growth of vegetation over the observed area, the real wetland and marshland observations may vary significantly from this model. In real observations, the vegetation cover over wetlands can take many varied form from grassland to thin tall plants to trees. This is illustrated in figure. In addition, the fractional area in a pixel covered by vegetation or completely bare flat water may also be varied. Therefore, a more thorough experimental characterization of vegetative growth and its relationship to the attenuation in a given pixel will have to be done before the model can be implemented.

5.1 Error Analysis and Cramer Rao Bound for the temporal resolution

Although the Doppler Delay Map coherent integrated power is a function $\Lambda(\Delta\tau)$, the width of Λ is not important in scatterometry applications. However, for altimetry applications, Λ determines the best achievable time resolution. The Cramer-Rao bound to give the limit of achievable time resolution is given by:

$$\sigma_\tau^2 \geq 1/SNR.\beta^2 \quad (6)$$

where SNR is the signal-to-noise ratio and β is the rms bandwidth i.e. a ratio of the squares of bandwidths of the receiver function and the transmitter as specified. The rms bandwidth can be understood in the terms that it is proportional to the achievable time resolution. If the rms bandwidth as specified is small, it would take longer for the signal to integrate to a given power over the coherent integration time. Consequently, the spatial resolution that can be achieved by the GNSS signal is a function of the SNR and the specified bandwidth of the receiver/transmitter.

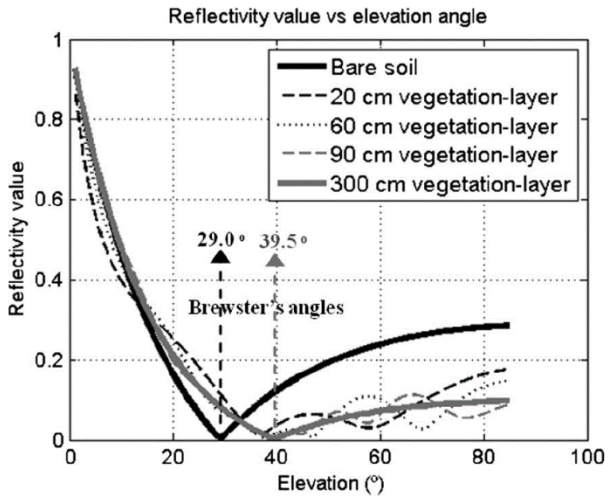

Figure 7: Equivalent reflectivity of the air + vegetation + soil model, as a function of the elevation angle, for different thickness of the vegetation layer.

To consider the achievable bandwidth, therefore, it is important to look at SNR values and the variables confounding them. There are two kinds of noise values that are added to the signal as it gets received and integrated at the receiver. These include the thermal noise and the fading noise. While most receivers model the thermal noise as additive white Gaussian noise, the fading noise has characteristics that are multiplicative. The fading fluctuations occur due to the unpredictable nature of constructive or destructive interference between multiple copies of the reflected signal. This kind of characteristics noise is also called 'speckle' noise and multiplies with the signal. There is no straight forward way to remove it, however, the SNR of the signal can be improved by increasing the coherent integration time of the signal at the cost of spatial resolution. Studies like [9] point to more detailed characteristics of the speckle noise and comments at its relationship with Brewster's angle. Some of its phase and fluctuation characteristics can be used for improved applications.

5.2 Next Steps

The next step to implementation and verification of the given model should take into account the CYGNSS data L1 DDM or power products and derive the three given derived products above. Next, already known geographic locations within the CYGNSS orbit for well-observed wetlands should be used to identify CYGNSS data products for the corresponding geophysical location. Then, the inversion of the products is used to verify against the ground truth observations of the given wetlands.

6.0 CONCLUSION

This paper has identified a set of parametric studies that has successfully observed and experimentally verified the parameters through a set of given measurements. While these studies are applied to a different set of application domain, principles are explained and extended to demonstrate that similar measurements can be used to identify model parameters for our proposed model of wetlands. Specifically, we suggest a three-parameter model using Interference Pattern Technique to identify three corresponding measurements in the observation domain that can be inverted to get the three proposed parameters in the parameter domain. The three measurements that can be inverted to their corresponding parameters are phase delay, Brewster's angle and number of notches in the reflected interference power. They can be inverted respectively to surface height (or high specular reflection binary hypothesis test), dielectric constant of the water and the height of the vegetative in the wetland.

7.0 REFERENCES

[1] M. Martin-Neira, P. Colmenarejo, G. Ruffini, and C. Serra, "Altimetry precision of 1 cm over a pond using the wide-lane carrier phase of GPS reflected signals," *Can. J. Remote Sens.*, vol. 28, no. 3, pp. 394–403, 2002.

[2] S. Gleason, "Space-based GNSS scatterometry: Ocean wind sensing using an empirically calibrated model," *IEEE Trans. Geosci. Remote Sens.*, vol. 51, no. 9, pp. 4853–4863, 2013.

[3] N. Rodriguez-Alvarez *et al.*, "Land geophysical parameters retrieval using the interference pattern GNSS-R technique," *IEEE Trans. Geosci. Remote Sens.*, vol. 49, no. 1 PART 1, pp. 71–84, 2011.

[4] M. Wiehl, R. Légrésy, and Dietrich R., "No Title," *Prog. Electromagn. Res.,* no. 40, pp. 177–205, 2003.

[5] J. T??yr??, A. Pietroniro, L. W. Martz, and T. D. Prowse, "A multi-sensor approach to wetland flood monitoring," *Hydrol. Process.*, vol. 16, no. 8, pp. 1569–1581, 2002.

[6] X. Na, S. Zang, Y. Zhang, and L. Liu, "Wetland mapping and flood extent monitoring using optical and radar remotely sensed data and ancillary topographical data in the Zhalong National Natural Reserve, China," *Proc. SPIE - Int. Soc. Opt. Eng.*, vol. 8893, p. 88931M, 2013.

[7] L. L. Bourgeau-Chavez, K. Riordan, N. Miller, M. Nowels, and R. Powell, "Remotely monitoring great lakes coastal wetlands with multi-sensor, multi-temporal sar and multi-spectral data," in *International Geoscience and Remote Sensing Symposium (IGARSS)*, 2008, vol. 1, no. 1.

[8] S. V. Nghiem *et al.*, "Wetland monitoring with Global Navigation Satellite System reflectometry," *Earth Sp. Sci.*, vol. 4, no. 1, pp. 16–39, Jan. 2017.

[9] V. U. Zavorotny, S. Gleason, E. Cardellach, and A. Camps, "Tutorial on remote sensing using GNSS bistatic radar of opportunity," *IEEE Geosci. Remote Sens. Mag.*, vol. 2, no. 4, pp. 8–45, 2014.

[10] D. Sahagian and J. Melack, "International Geosphere-Biosphere Programme-Global Analysis, Interpretation and Modelling (IGBP-GAIM)," 1996.

[11] A. Woodward *et al.*, "Climate change and health: On the latest IPCC report," *Lancet*, vol. 383, no. 9924, pp. 1185–1189, 2014.

[12] R. Brakenridge and E. Anderson, "MODIS-based flood detection, mapping and measurement: the potential for operational hydrological applications," *Transbound. Floods Reducing Risks Through Flood Manag. SE - 1*, vol. 72, pp. 1–12, 2006.

[13] E. Cardellach, F. Fabra, O. Nogués-Correig, S. Oliveras, S. Ribó, and A. Rius, "GNSS-R ground-based and airborne campaigns for ocean, land, ice, and snow techniques: Application to the GOLD-RTR data sets," *Radio Sci.*, vol. 46, no. 6, Dec. 2011.

[14] R. N. Treuhaft, S. T. Lowe, C. Zuffada, and Y. Chao, "2-cm GPS altimetry over Crater lake," *Geophys. Res. Lett.*, vol. 28, no. 23, pp. 4343–4346, 2001.